Optical and Quantum Electronics (2022) 54:824
https://doi.org/10.1007/s11082-022-04161-1

Comparison between CrZO and AlZO thin layers and the effect of doping on the lattice properties of zinc oxide

Dikra Bouras[1] · **Mohammed Rasheed**[2]

Received: 20 April 2022 / Accepted: 1 September 2022

Abstract
This work aims to study and compare the effect of doping with two elements (chromium and aluminum) and the addition ratio (0, 2, 5, and 8)% on the structural, morphological, surface, optical, and photocatalysis properties of zinc oxide thin films. Thin layers were prepared using the sol–gel deposition dip-coating technique on a glass slide. The X-ray analysis proved that the crystal structure of ZnO is of the type wurtzite; its effect was evident through a decrease in the intensity of the peaks and their shift towards the most prominent angles. The results of AFM showed an increase in the surface roughness during doping, as it gave a more effective surface during the use of Al element than during the use of Cr. The shape of the spherical grains was confirmed by the SEM device, where we obtained a larger size of the grains with a porous surface in the case of doping with Al compared with Cr. Based on the transmittance spectrum, the energy gap of the samples was calculated, which was found to have increased with doping, where ZnO had an energy gap of 3.23 eV, and its value in the case of doping with 8% of Cr and Al reached (3.24 and 3.29) eV, respectively. A good surface for the AlZO sample made it more catalytic. It gave it the most significant gradient rate, estimated at 55.23% during a time of 180 min, compared to the CrZO sample, which was estimated at 32.99% during the same period.

Extended author information available on the last page of the article

Published online: 10 October 2022

Graphical abstract

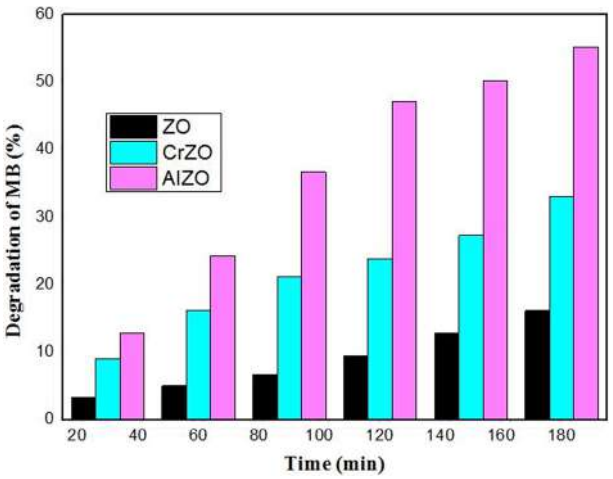

Keywords AlZO · CrZO · Dip-coating · Energy gap · Nanotechnology

1 Introduction

The study of the physical properties of thin layers is of great interest to the scientific and industrial community (Maldonado and ArvidsStashans 2010). Transparent and conductive oxides (TCO) are remarkable materials in many fields. Their dual property, electrical conductivity, and transparency in the visible make them ideal candidates for optoelectronic and photovoltaic applications (Hichou et al. 2004).

Zinc oxide is considered one of the most promising materials. There have been reports of photoelectric devices like thin films of $CsPbBr_3$ perovskite with ZnO nanoparticles on them to improve random lasing (Li et al. 2017a). Efficiency enhancement of ZnO/Cu_2O solar cells with well-oriented and micrometer grain-sized Cu_2O films (Zang 2018). Femtosecond laser direct writing of microholes on roughened ZnO for output power enhancement of InGaN light-emitting diodes (Zang et al. 2016). NH_4Cl-modified ZnO for high-performance $CsPbIBr_2$ perovskite solar cells via low-temperature process (Wang et al. 2020). The Enhanced photoresponse of self-powered perovskite photodetector based on ZnO nanoparticles decorated $CsPbBr_3$ films (Li et al. 2017b).

At the forefront of these materials, ZnO has exciting properties. It is considered one of the materials that have been studied and taken care of for a long time, mainly due to its broad uses in various fields. It is from the TCO family, considered a semiconductor material because it is an excellent transparent conductive oxide. It is characterized by high electrical conductivity and weak absorption intensity in visible and near-infrared rays. It is relied upon in detecting other gases because it is non-toxic and is found in abundance on the ground—electronic devices are damaged when a sudden rise in tension occurs. In the photovoltaic field, ZnO is considered one of the most promising materials for manufacturing blue-light emitting dipoles (Jin et al. 2009). It is the ideal carrier for the growth of thin

layers. ZnO is a semiconductor belonging to the II-VI column with a directly forbidden bandwidth of 373 eV. At standard temperature.

In this field, zinc oxide is considered one of the most studied materials, whether in its pure state or tainted with various oxides, due to the significant changes observed in its electrical, optical, magnetic, and electrostatic properties ("The structural properties of Al doped ZnO 2011). It is characterized by a natural negative electrical conductivity caused by zinc inter-atoms. The conductivity values of zinc oxide can change in the case of doping so that its value can be between (3.3 and 3.9) eV (Lee et al. 2020; Aljawfi et al. 1065; Chang et al. 2014). These reasons motivated us for this choice, during which we developed thin layers of ZnO to study their optical, structural and electrical properties (Kandjani et al. 2011).

According to studies, the preparation method dramatically affects the quality and properties of the obtained solutions, so the researchers emphasized diversifying the methods of preparing these materials. We mention, for example, the process of thermal spraying and evaporation at low temperature, water bath, and chemical preparation (Sol–Gel) that we relied on in the study. Among the dip-coating technique we used, it has the advantage of being a simple and economical method (Al-Hardan et al. 2013).

The elements used as impurities for doping zinc oxide often belong to columns III (III) and IV (IV) of the periodic table of the ingredients (Mingredients's table). In this case, the added atoms occupy the positions of zinc atoms in the crystal lattice. In the case of doping with elements from the seventh column (VII) of the periodic table of the elements, the added detailscupy the positions of the oxygen atoms in the lattice. Therefore, there are significant results related to doping ZnO with various oxides; this took an important part and space in our study, where we used zinc oxide dotted with chromium and aluminum oxides.

This study prepared thin layers of ZnO doped with different percentages of chromium and aluminum. Then the structural, optical morphological, and catalytic properties of these samples were studied, and their effect on the crystal lattice of zinc oxide was seen. Also, visible light was used instead of a UV irradiation lamp as the light source used in previous studies. Thus, a light source was wholly abandoned and works on natural sources such as the sun or visible light, which does not require any effort.

2 Experimental procedure

2.1 Materials

For the preparation of the active layers used, the following chemical compounds: zinc acetate dehydrate [$(Zn(CH_3COO)_2.2H_2O)$] (98%; Sigma-Aldrich), monoethanolamine [C_2H_7NO] (MEA; 99%; Merck), chromium chloride [$CrCl_3$] (98%; Sigma-Aldrich), and Aluminum Chloride [$AlCl_3$] (99.999%; Sigma-Aldrich). For photocatalysis application, Methylene blue [$C_{16}H_{18}ClN_3S$] (≥ 95%; Sigma-Aldrich) has been used.

2.2 Preparation of thin layers using Sol–Gel technique

A solution consisting of m = 1.2 g of zinc acetate ($C_4H_6O_4Zn.2H_2O$) dissolved in 20 ml of absolute ethanol. The catalyst (MEA) monoethanolamine is added as a catalyst and has been used for preparation. A chromium chloride ($CrCl_3$) and aluminum chloride ($AlCl_3$) as a dopant in a ratio of (2, 5, and 8)% have been used too. The solutions are placed over

a magnetic stirrer at 70 °C for two hours until the mixture becomes homogeneous and transparent.

After depositing 25 layers of each species, the samples were annealed at 500 °C for 2 h.

The main objective of using the aluminum chloride compound $AlCl_3$ at the beginning of the preparation of the solution is because it reacts strongly with water and emits fumes in the humid atmosphere. It is known for its anhydrous form and melting point of 190 °C, which makes it subject to evaporation and leaves behind holes and interstitial spaces because the heat treatment temperature of the samples is 500 °C.

3 Results and discussion

3.1 Structural characteristics

X-ray diffraction schemes for thin layers prepared by Sol–gel (dip-coating) of pure ZnO and doped with 2, 5, and 8% for chromium and aluminum are shown in Fig. 1a and b. The results show that the obtained ZnO films are polycrystalline with a hexagonal structure of the Wurtzite type. Figure 1 shows two peaks of great intensity at angles 34.35 and 36.15°,

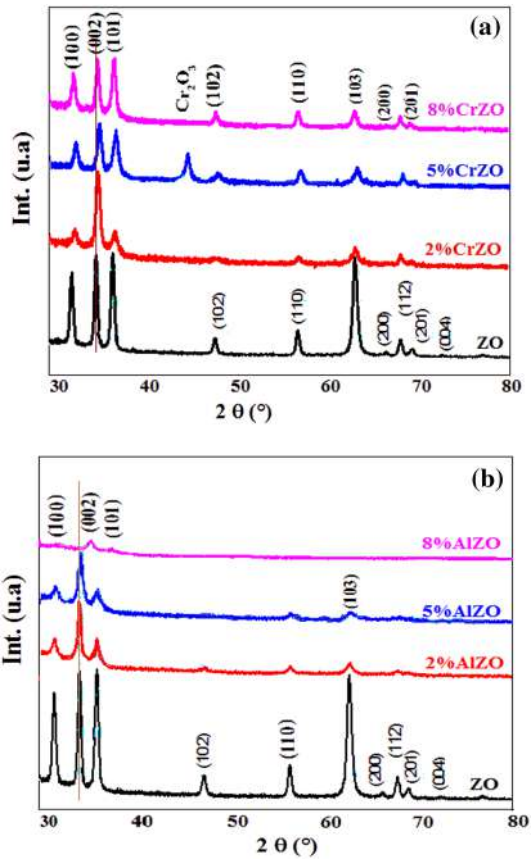

Fig. 1 X-ray diffraction spectra of ZnO samples doped with different percentages of **a** chromium and **b** aluminum

corresponding to the (002) and (101) planes, respectively; this explains that zinc oxide layers grow and compact significantly according to these two levels.

Nevertheless, when doping was done, the intensity of the two peaks in these levels decreased as the amount of chromium added to ZnO went up Fig. 1a because the crystal structure of the zinc oxide lattice was changed, and a new phase, Cr_2O_3, formed at an angle of 47.45°.

In the case of doping with aluminum, the peaks seem to get smaller, with most of them going away; this is called "crystallization," and the decrease gets more prominent, bringing the percentage of Al goes up Fig. 1b.

On the other hand, there is a shift of the X-ray spectra towards larger angles due to the rearrangement of crystals deposited during doping for each of the aluminum ($Al^{+3} = 0.54$ A^o) and chromium ($Cr^{+3} = 0.615$ A^o), which has an ionic diameter less than zinc ($Zn^{+2} = 0.74$ A^o) to creating compressive stress on the crystal lattice (Bouras et al. 2017, 2021). It leads to an increase in the energy gap.

3.2 Morphological characteristics

3.2.1 AFM

The surface morphology of undoped ZnO and doped with chromium (CrZO), and aluminum (AlZO) thin films deposited on glass substrates by atomic force microscopy in the area (3×3) μm^2 have been studied and analyzed. The relationship between the shape of the grains and the surface roughness of the membranes is shown by the atomic force microscopy images in three-nanometer dimensions, as shown in Fig. 2.

The results show that the structure of zinc oxide is in the form of mountains with a broad base and a sharp peak, where the average surface roughness is 188.3 nm. During doping with chromium, we notice a difference in the surface shape from one area to another with a more cylindrical growth of the two phases and their protrusion in the directions (002) and (101); the results of XRD confirmed this matter. The surface roughness reached 214.4 nm after adding an 8% concentration of chromium (Table 1).

When it comes to the layers of ZnO-doped Al (ALZO), the size of the grains gets more prominent as the width of the mountains gets more significant, which makes the surface rougher because there are open spaces between the grains. The average surface roughness after doping with 8% of the aluminum was 215 nm; this increase gives a more effective surface than the previous two.

Aluminum makes the grains bigger, which can be explained by the fact that aluminum is present at the grain boundary and on the surface of the crystalline lattice nanoparticles of ZnO. So, we can say that doping significantly affects the granules' growth and the crystals' size.

3.2.2 SEM

Figures 3a, b, and c taken by scanning electron microscopy shows the upper surface of the morphology of the ZnO, CrZO, and AlZO layers. The method used to prepare the thin layers affects the increase in the atomic mobility of the lattice and facilitates the incorporation of oxygen to form ZnO crystals. The ZnO layer in Fig. 3a shows a stable surface with a small, spherical nano-granular size of 810 nm.

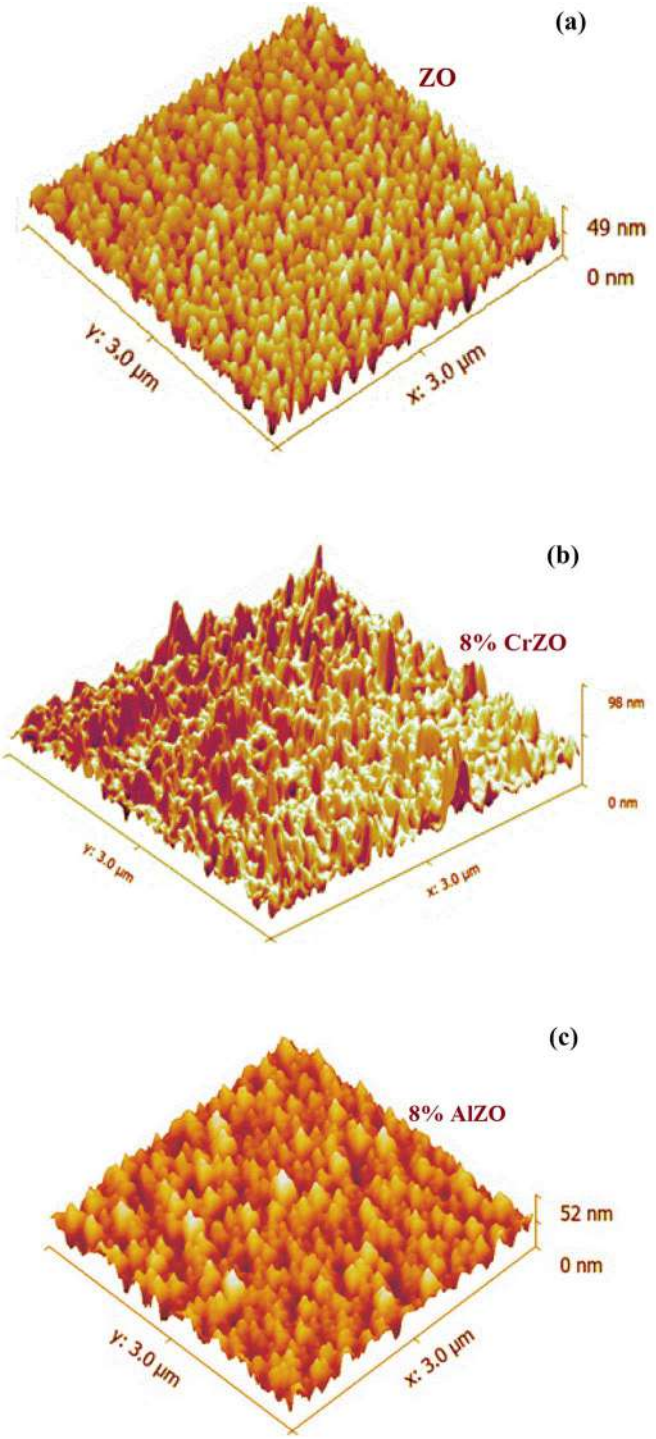

Fig. 2 Three-dimensional (3D) AFM images of **a** ZnO, **b** 8% Cr-doped ZnO, and **c** 8% Al-doped ZnO

Table 1 The roughness of the prepared samples

Samples	ZO	CrZO	AlZO
Surface roughness (RMS) (nm)	188.3	214.4	215

Doping significantly affects the shape of the upper surface, which was observed in Fig. 3b and c. The CrZO layer in Fig. 3b has a rough surface with irregularly distributed fine spherical particles spread over the entire surface with a size of 880 nm; at the same time, the AlZO layers in Fig. 3c also show a rougher and porous surface with nano-sized spherical grains, where the average size of the particles was 1520 nm, which is due to the effect of doping with aluminum, which gave a more practical surface.

The source of the primary oxides is a big part of making pores on the sample's surface. Aluminum chloride has been used as the source, not by chance, because it evaporates and melts at different rates than other sources (for example, aluminum acetate or aluminum nitrate). After heat treatment at 500 °C, they were allowed to evaporate the aluminum element leaving behind pores and holes along the sample's surface. The results of X-rays have proved this by not showing any spectrum of aluminum oxide. It can also be attributed to the small additional amount, estimated at 8 wt.%.

3.3 Optical properties

3.3.1 Optical transmittance and gap energy

The optical properties of undoped and Cr/Al-doped ZnO thin films were determined from the transmission measurement range of (200–900) nm. In Fig. 4a, we can see that the thin layers of CrZO present an average transmittance varying between (60 and 80) %, with a maximum transmittance measured in the thin layers doped with 2% Cr. On the other hand, it ranged between (70 and 90) % for the AlZO thin layers, where the highest transmittance value was determined for 5% of aluminum in Fig. 4b. We also note that the transmittance is influenced by the doping concentration, where it decreased when the doping concentration energy gap was calculated from the slope of the curve $(\alpha h\upsilon)^2$ in terms of $(h\upsilon)$ according to the following relationship (Bouras et al. 2017, 2018, 2021; Rasheed and Barillé 2017b):

$$h\upsilon = (\alpha h\upsilon)^2 \tag{1}$$

where α is the absorption coefficient, hυ is the photon energy, and E_g is the optical bandwidth.

The effect of Cr and Al doping on the absorption limit is shown in Fig. 5a and b. A shift in the absorption limit is observed when the Cr and Al concentration increases. The calculated optical gap of the samples increases with increasing Al concentration, from 3.23 eV for undoped ZnO films to 3.29 eV for ZnO doped with 8% Al in Fig. 5b. At the same time, it reaches an energy gap of 3.24 eV at the same ratio during doping with chromium. This absorption shift of CrZO and AlZO nanocrystalline films can be explained by the Burstein-Moss effect (Saidani et al. 2017; Enneffati et al. 2018; Dkhilalli et al. 2018; Rasheed and Barillé 2017a, c) while assuming the increase in carrier concentration that blocks the lowest states in the conduction band.

Reducing the average size of the crystals under the influence of ZnO lattice deformation can modify its electronic structure, thereby increasing the optical gap (Ali et al. 2017). The

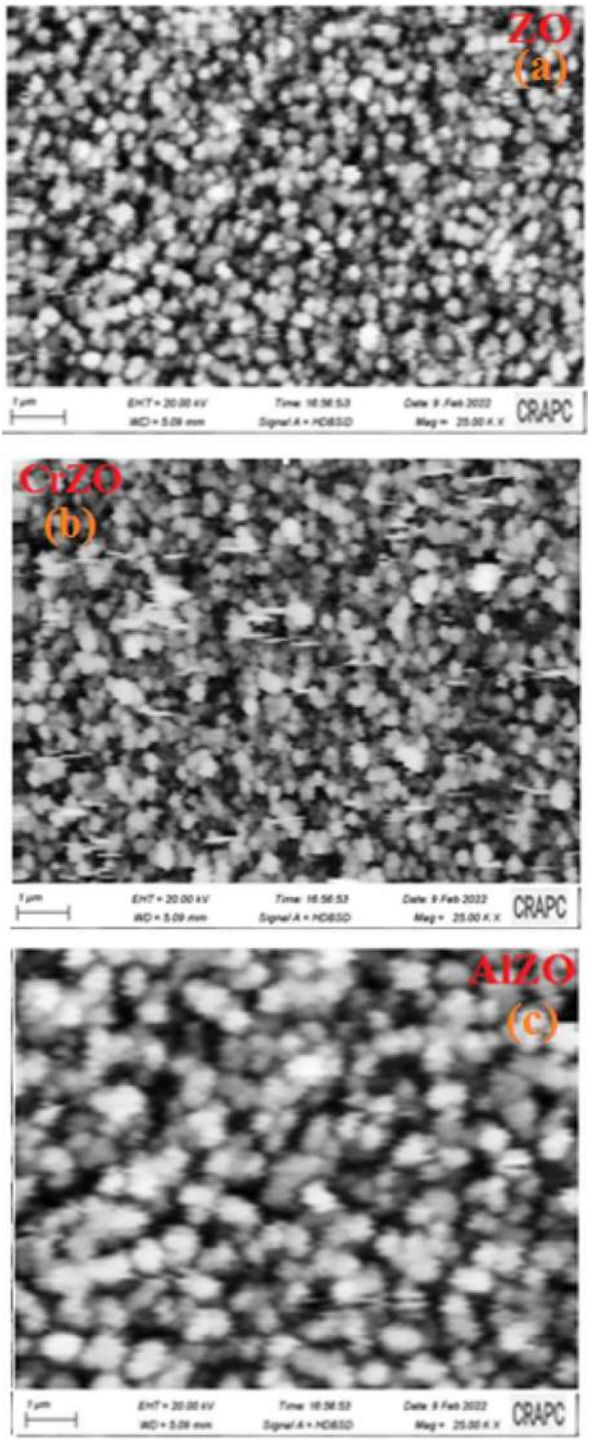

Fig. 3 SEM images of thin layers **a** ZnO **b** 8% Cr doped ZnO, and **c** 8% Al-doped ZnO

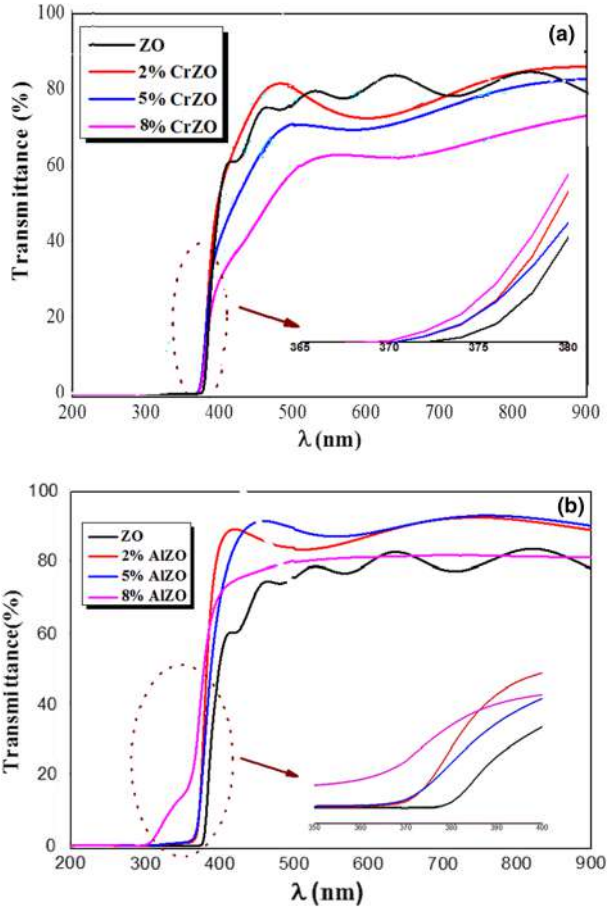

Fig. 4 Optical transmittance spectra obtained for the thin layers of ZnO produced with different doping of Al and Cr

micro deformation can cause changes in the spacing between atoms in semiconductors, which in turn also affect the gap energy value (Swanepoel 1983). It was found that the gap widening noticeably in the sample grafted with aluminum element is due to an increase in compressive stress along the [002] c axis, which is consistent with our results, which show a significant increase in defects and thus a decrease in the crystal quality of the layers. It can be said that the optical energy gap is directly proportional to the size of the crystal grains, as it appears to be a deviation in the absorption limit toward lower energy levels, and this is explained by the quantum warming phenomenon (Ali et al. 2017; Swanepoel 1983).

3.4 Photocalytic perform

To study and know the effect of doping with aluminum and chromium on thin films of zinc oxide in the field of photocatalysis, the gradient ratio analysis of methylene blue (MB) solution with a concentration of 4 mg/L was studied. The process was carried out by placing the three samples, ZO, CrZO, and AlZO, in 40 ml of the prepared solution (MB). Every

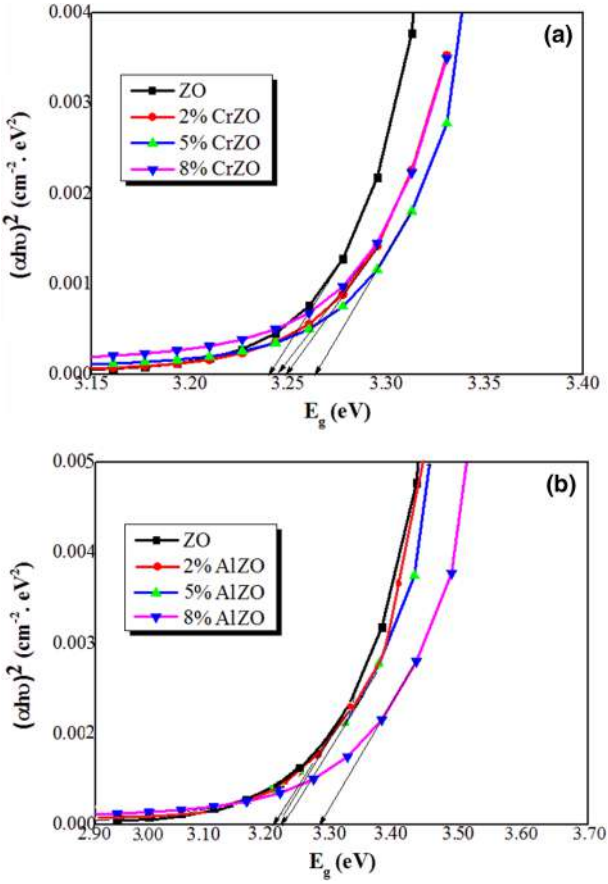

Fig. 5 Energy gap values for samples before and after doping with Cr and Al

30 min and 0.3 ml of the solution is taken to measure the absorbance of the UV–Visible device.

Figures 6a, b, and c shows the absorbance spectra in terms of wavelength in the range of (500–800) nm with a maximum absorbance value of 664 nm. From these spectra, the gradient ratio of the three solutions was calculated while using the prepared samples as a function of time in Fig. 6 using the following relationship (Bouras et al. 2017, 2018, 2021; Sukee et al. 2017):

$$\text{Degradation } (\%) = \frac{C_0 - C}{C_0} \times 100\% \tag{2}$$

where C_0 is the concentrations before illumination and C is the concentrations after illumination.

For the ZO sample without doping, the solution gradient reached 16.16% over some time of 180 min. Figure 7 shows the scaling process that takes place slowly in the case of ZO. In the case of doping zinc oxide with 8% chromium (8% Cr doped ZnO), an increase in the degradation rate, reaching 32.99% within 180 min, has been noticed. In comparison, doping with aluminum (8% Al-doped ZnO) was very effective compared to the previous two eyes, where the gradient ratio was estimated at 55.23% during the same time in Fig. 7.

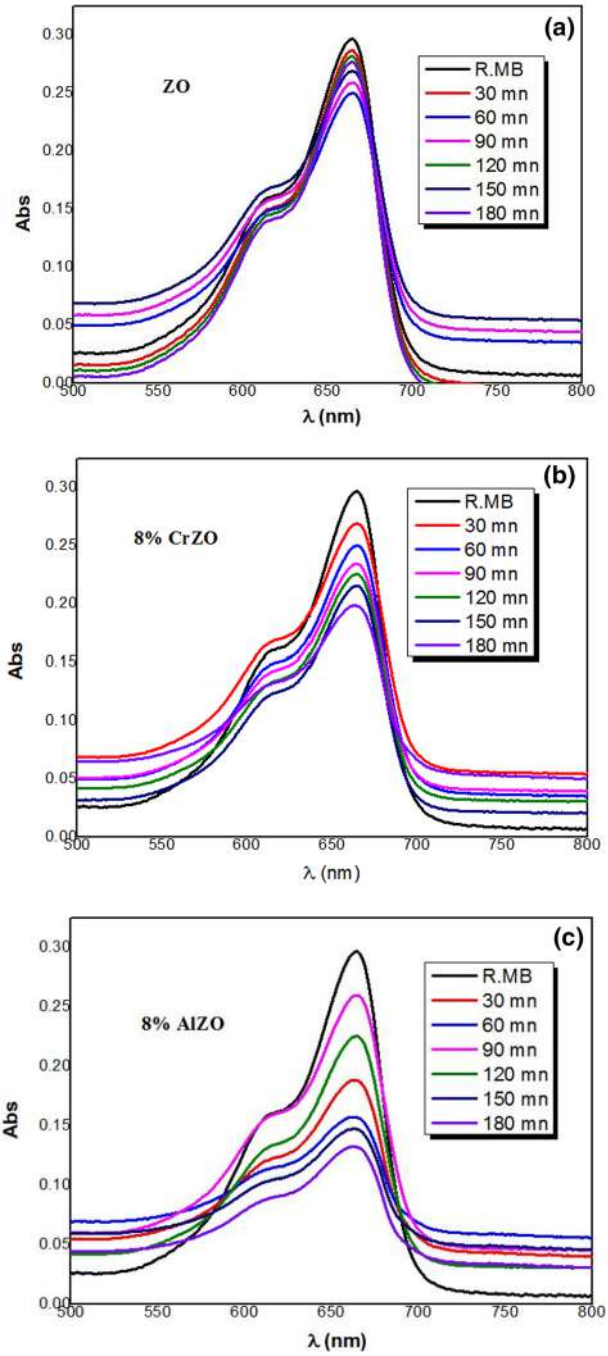

Fig. 6 Absorbance spectra of MB solution gradient using thin layers of samples: **a** ZnO, **b** 8% Cr doped ZnO, and **c** 8% Al-doped ZnO

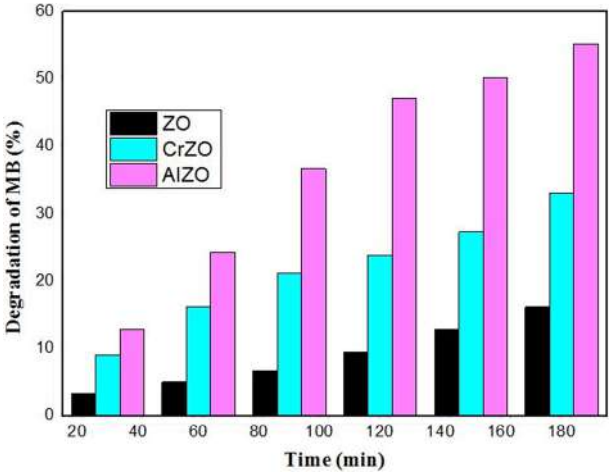

Fig. 7 The solution MB's degradation during the measured times

It is noted that the higher the additional percentage, the greater the effectiveness of breaking down the harmful organic pigments in the water during photocatalysis.

Considering that the process occurs in the presence of visible light without an additional stimulus and with thin layers of shallow thickness on glass substrates, the time at which the dissolution rate reaches a high percentage increases because the longer we leave the sample inside the solution for a longer time, the higher the rate of decomposition.

The samples that were worked during the photocatalytic process with lengths (2.5×2) cm^2 are placed in 40 ml of methylene blue solution (which is a significant amount compared to the sample size), knowing that the precipitated layer is skinny. Its effectiveness is more minor than tablets with larger fish; therefore, the larger the sample size, the greater the stimulation and faster decomposition. Thus, time is of great importance in this process.

The widening of the energy gap also contributed to decreasing the decay rate with increasing time, and this is because the level of electrons that move to the conduction threshold is lower, and therefore its conductivity decreases. Knowing that the creation of (electron/hole) gives $\cdot O_2^-$ and $\cdot OH^-$, which works to dissociate and give white light to the polluted solution MB.

4 Conclusion

This study focused on identifying properties that could improve the quality of materials for use in optical and photocatalysis. To do this, we prepared thin layers of pure ZnO doped with aluminum and chromium at concentrations of (2, 5, and 8) %. After adding doping, the structural analysis of zinc oxide proved that there was a shift towards larger angles and a distortion in the crystal structure by occupying Cr^{+3} and Al^{+3} atoms in the ZnO lattice. This pressure increased the energy gap during doping, which changed from 3.23 eV (before doping) to 3.24 eV in the case of doping with Cr and 3.29 eV in the case of doping with Al. The morphology of the samples showed that the particles have a spherical shape of the nano rank, where the effect of aluminum was apparent by obtaining a larger particle size and a porous surface. The samples proved their effectiveness in photocatalysis application, where the dissolution rate reached 55.23% within 180 min while doping with 8% Al

because it had a more practical surface. In comparison, it came to 32.99% during the same time for 8% Cr.

Acknowledgements This work has been supported by the Laboratory of Active Components and Materials (LACM) of Larbi Ben M'hidi University—Oum El Bouaghi, Algeria.

Funding The authors have not disclosed any funding.

Data Availability The data supporting this work are available upon reasonable request from the authors.

Declarations

Conflict of Interest The authors declare that they have no conflict of interest.

References

Al-Hardan, N.H., Abdullah, M.J., Abdul Aziz, A.: Performance of Cr-doped ZnO for acetone sensing. Appl. Surface Sci. **270**, 480–485 (2013)

Ali, D., Butt, M.Z., Arif, B., Al-Sehemi, A.G., Al-Ghamdi, A.A., Yakuphanoglu, F.: Li induced enhancement in c-axis orientation and its effect on structural, optical, and electrical properties of ZnO thin films. Mater. Res. Express **4**(2), 026405 (2017)

Aljawfi, R.N., Rahman, F., Batoo, K.M.: Effect of grain size and boundary defects on electrical and magnetic properties of Cr doped ZnO nanoparticles. J Molecular Structure **1065**, 199–204 (2014)

Bouras, D., Mecif, A., Mahdjoub, A., Harabi, A., Zaabat, M., Benzitouni, S., Regis, B.: Photocatalytic degradation of orange II by active layers of Cu-doped ZnO deposited on porous ceramic substrates. J. Ovonic Res. **13**(5), 271–281 (2017)

Bouras, D., Mecif, A., Barillé, R., Harabi, A., Rasheed, M., Mahdjoub, A., Zaabat, M.: Cu: ZnO deposited on porous ceramic substrates by a simple thermal method for photocatalytic application. Ceram. Int. **44**(17), 21546–21555 (2018)

Bouras, D., Mecif, A., Harabi, A., Barillé, R., Mahdjoub, A., Zaabat, M.: Economic and ultrafast photocatalytic degradation of orange II using ceramic powders. Catalysts **11**(733), 1–22 (2021)

Chang, C.-J., Chen, J.-K., Yang, T.-L.: Cr-doped ZnO based NO2 sensors with high sensitivity at low operating temperature. J. Taiwan Inst. Chem. Eng. **45**(4), 1876–1882 (2014)

Dkhilalli, F., MegdicheBorchani, S., Rasheed, M., Barille, R., Shihab, S., Guidara, K., Megdiche, M.: Characterizations and morphology of sodium tungstate particles. Royal Soc. Open Sci. **5**(8), 172214 (2018)

El Hichou, A., Addou, M., Bougrine, A., Dounia, R., Ebothé, J., Troyon, M., Amrani, M.: Cathodoluminescence properties of undoped and Al-doped ZnO thin films deposited on glass substrate by spray pyrolysis. Mater. Chem. Phys. **83**(1), 43–47 (2004)

Enneffati, M., Louati, B., Guidara, K., Rasheed, M., Barillé, R.: Crystal structure characterization and AC electrical conduction behavior of sodium cadmium orthophosphate. J. Mater. Sci.: Mater. Electron. **29**(1), 171–179 (2018)

Jin, H.-J., Song, M.-J., Park, C.-B.: A novel phenomenon: p-Type ZnO: Al films deposited on n-Si's findings his study substrate. Physica B **404**(8–11), 1097–1101 (2009)

Kandjani, A.E., Tabriz, M.F., Moradi, O.M., Mehr, H.R., Kandjani, S.A., Vaezi, M.R.: An investigation on linear optical properties of dilute Cr doped ZnO thin films synthesized via sol–gel process. J. Alloys Compounds **509**(30), 7854–7860 (2011)

Lee, M., Park, Y., Kim, K., Hong, J.: Influence of sputtering conditions on the properties of aluminum-doped zinc oxide thin film fabricated using a facing target sputtering system. Thin Solid Films **703**, 137980 (2020)

Li, C., Zang, Z., Han, C., Zhiping, Hu., Tang, X., Juan, Du., Leng, Y., Sun, K.: Highly compact CsPbBr 3 perovskite thin films decorated by ZnO nanoparticles for enhanced random lasing. Nano Energy **40**, 195–202 (2017a)

Li, C., Han, C., Zhang, Y., Zang, Z., Wang, M., Tang, X., Jihe, Du.: Enhanced photoresponse of self-powered perovskite photodetector based on ZnO nanoparticles decorated CsPbBr 3 films. Sol. Energy Mater. Sol. Cells **172**, 341–346 (2017b)

Maldonado, F., Stashans, A.: Al-doped ZnO: Electronic, electrical and structural properties. J. Phys. Chem. Solids. **71**(5), 784–787 (2010)
Rasheed, M., Barillé, R.: Optical constants of DC sputtering derived ITO, TiO2 and TiO2: Nb thin films characterized by spectrophotometry and spectroscopic ellipsometry for optoelectronic devices. J. Non-Crystalline Solids **476**, 1–14 (2017a)
Rasheed, M., Barillé, R.: Room temperature deposition of ZnO and Al: ZnO ultrathin films on glass and PET substrates by DC sputtering technique. Opt. Quant. Electron. **49**(5), 1–14 (2017b)
Rasheed, M., Barillé, R.: Comparison the optical properties for Bi_2O_3 and NiO ultrathin films deposited on different substrates by DC sputtering technique for transparent electronics. J. Alloy. Compd. **728**, 1186–1198 (2017c)
Ri, K.H., Wang, Y., Zhou, W. L., Gao, J. X., Wang, X. J., Jun, Y.: The structural properties of Al doped ZnO films depending on the thickness and their effect on the electrical properties. Appl. Surface Sci. **258**(4), 1283–1289 (2011)
Saidani, T., Zaabat, M., Aida, M.S., Barille, R., Rasheed, M., Almohamed, Y.: Influence of precursor source on sol-gel deposited ZnO thin films properties. J. Mater. Sci.: Mater. Electron. **28**(13), 9252–9257 (2017)
Sukee, A., Kantarak, E., Singjai, P.: Preparation of aluminum doped zinc oxide thin films on glass substrate by sparking process and their optical and electrical properties. J. Phys: Conf Ser **901**(1), 012153 (2017)
Swanepoel, R.: Determination of the thickness and optical constants of amorphous silicon. J. Phys. E: Sci. Instrum. **16**(12), 1214 (1983)
Wang, H., Cao, S., Yang, B., Li, H., Wang, M., Xiaofei, H., Sun, K., Zang, Z.: NH4Cl-modified ZnO for high-performance CsPbIBr 2 perovskite solar cells via low-temperature process. Solar Rrl **4**(1), 1900363 (2020)
Zang, Z.: Efficiency enhancement of ZnO/Cu_2O solar cells with well oriented and micrometer grain sized Cu_2O films. Appl. Phys. Lett. **112**(4), 042106 (2018)
Zang, Z., Zeng, X., Jihe, Du., Wang, M., Tang, X.: Femtosecond laser direct writing of microholes on roughened ZnO for output power enhancement of InGaN light-emitting diodes. Opt. Lett. **41**(15), 3463–3466 (2016)

Authors and Affiliations

Dikra Bouras[1] · Mohammed Rasheed[2]

✉ Mohammed Rasheed
rasheed.mohammed40@yahoo.com; mohammed.s.rasheed@uotechnology.edu.iq

[1] Laboratory of Active Components and Materials (LCAM), University of Larbi Ben M'hidi, 04000 Oum El Bouaghi, Algeria

[2] Applied Sciences Department, University of Technology, Baghdad, Iraq